Structure and linear viscoelasticity of flexible polymer solutions: comparison of polyelectrolyte and neutral polymer solutions

Ralph H. Colby

Abstract The current state of understanding for solution conformations of flexible polymers and their linear viscoelastic response is reviewed. Correlation length, tube diameter, and chain size of neutral polymers in good solvent, neutral polymers in θ-solvent, and polyelectrolyte solutions with no added salt are compared as these are the three universality classes for flexible polymers in solution. The 1956 Zimm model is used to describe the linear viscoelasticity of dilute solutions and of semidilute solutions inside their correlation volumes. The 1953 Rouse model is used for linear viscoelasticity of semidilute unentangled solutions and for entangled solutions on the scale of the entanglement strand. The 1971 de Gennes reptation model is used to describe linear viscoelastic response of entangled solutions. In each type of solution, the terminal dynamics, reflected in the terminal modulus, chain relaxation time, specific viscosity, and diffusion coefficient are reviewed with experiment and theory compared. Overall, the agreement between theory and experiment is remarkable, with a few unsettled issues remaining.

Keywords Polymer solution · Relaxation time · Reptation · Dynamic moduli · Viscoelasticity · Semidilute polymer solution

Dedicated to the memory of Professor Pierre-Gilles de Gennes; gourou magnifique et inspiration éternelle.

R. H. Colby (✉)
Materials Science and Engineering, The Pennsylvania State University, University Park, PA 16802, USA
e-mail: rhc@plmsc.psu.edu

Introduction

In the mid-1970s, the structure and dynamics of polymer solutions was unclear. Empirical correlations for the viscosity of neutral polymer solutions, involving molar mass and concentration, were well established (Berry and Fox 1968; Graessley 1974), but genuine understanding was sorely lacking. De Gennes provided the key missing structural component in neutral polymer solutions—a complete understanding of the concentration dependence of the correlation length and why it cannot depend on molar mass, for both universality classes (athermal solvent and θ-solvent) and everything in between (Daoud et al. 1975; de Gennes 1979; Rubinstein and Colby 2003). He also provided the insight needed to begin understanding dynamics (de Gennes 1976a, b, 1979). Polyelectrolyte solutions were even less understood in the mid-1970s as the competing effects of charge repulsion and counterion condensation on chain conformation and solution structure were just beginning to be understood (Oosawa 1971; Katchalsky 1971). De Gennes again provided the key missing structural component for polyelectrolyte solutions—a complete understanding of the concentration dependence of the correlation length and blazed the trail for understanding their dynamics in a paper that radically changed this field (de Gennes et al. 1976). In this review, we summarize those advances and the current state of understanding of structure and dynamics of polyelectrolyte and neutral polymer solutions. It is intended to compliment and bring together excellent recent reviews of neutral polymer solutions (Teraoka 2002; Rubinstein and Colby 2003; Graessley 2003, 2008) and polyelectrolyte solutions (Dobrynin and Rubinstein 2005), leaving the reader with a complete picture.

One reason such a comparison of polyelectrolyte and neutral polymer solutions has not yet been made is that the natural concentration units differ. In polyelectrolyte solutions, the charge on the chain plays a vital role and the natural concentration unit is the number density of chemical repeat units in the chain c_n, typically with units of moles of monomer per liter. In solutions of neutral polymers, two other natural concentration measures are used routinely, mass concentration of polymer c (i.e., g/mL) and volume fraction of polymer ϕ. In this review, all three concentration units are necessarily utilized.

Solution conformations

In dilute solutions, polymers exist as individual chains, with conformations summarized schematically in Fig. 1. For neutral polymers in θ-solvent, the chains are random walks, and this individual chain statement is only mostly true as when two chains approach each other (with zero net excluded volume), there is only three-body repulsion and some temporary association occurs that influences properties such as the Huggins coefficient (Bohdanecky and Kovar 1982; Xu et al. 1984). With zero net excluded volume, two chains are able to overlap occasionally in dilute θ-solvent and temporarily entangle (Semenov 1988). For neutral polymers in good solvent, or in the extreme limit of athermal solvent (Rubinstein and Colby 2003), the excluded volume

between chains keeps them apart in dilute solution and makes them adopt a somewhat expanded self-avoiding walk conformation. In polyelectrolyte solutions without salt, charge repulsion dominates, and this keeps the chains apart and stretches the chain into a directed random walk of electrostatic blobs (de Gennes et al. 1976; de Gennes 1979; Dobrynin et al. 1995) in dilute solution; each step along the chain axis is directed by charge repulsion, while the two orthogonal directions have the meanderings of random walks.

As concentration is raised, the conformations of individual chains start to overlap each other at the overlap concentration, defined as the point where the concentration within a given dilute conformation's pervaded volume is equal to the solution concentration. In terms of number density of Kuhn monomers (Rubinstein and Colby 2003), the overlap concentration $c^* \approx N/R_{\text{dilute}}^3$, where N is the number of Kuhn monomers in the chain and R_{dilute} is the dilute solution size of the chain. In θ-solvent, we use the ideal coil end-to-end distance $R_0 = bN^{1/2}$ (b is the Kuhn monomer size), making c^* proportional to $N^{-1/2}$. In good solvent, we use the Flory end-to-end distance $R_F = bN^{0.588}$ of the self-avoiding
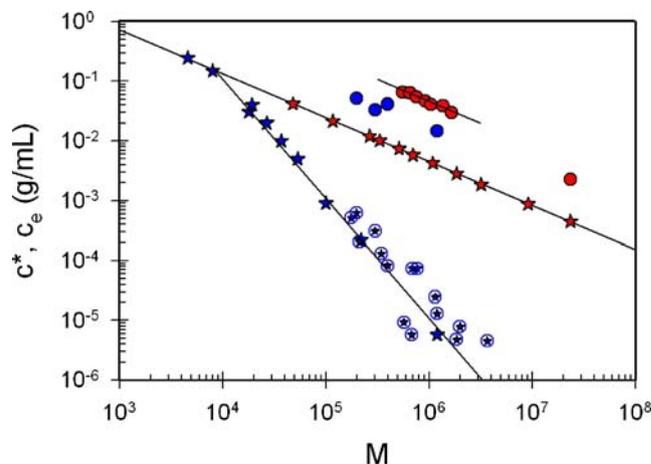
Fig. 2 Comparison of overlap concentrations and entanglement concentrations for neutral polymer solutions in good solvent; *red stars* overlap concentrations, c^*, of polystyrene in toluene (Kulicke and Kniewske 1984); *red circles* entanglement concentrations, c_e, of polystyrene in toluene (Onogi et al. 1966 viscosity data fit to power laws with slope 1.3 and 3.9, highest M point from Kulicke and Kniewske 1984) with polyelectrolyte solutions in water with no added salt; *blue stars* overlap concentrations, c^*, of sodium poly(styrene sulfonate) from SAXS (Kaji et al. 1988); *stars with blue circles* overlap concentrations, c^*, of sodium poly(styrene sulfonate) from viscosity (Boris and Colby 1998); *blue circles* entanglement concentrations of sodium poly(styrene sulfonate) from viscosity (Boris and Colby 1998). *Lowest line* has slope -2, expected for c^* of polyelectrolyte solutions with no salt; *middle line* is Mark–Houwink fit with slope -0.7356 (predicted slope is -0.76); *upper line* has same slope going through neutral c_e data

Fig. 1 Conformations of polymers in dilute solution. Neutral polymers in poor solvent collapse into dense coils with size $\approx bN^{1/3}$ (*purple*). Neutral polymers in θ-solvent are random walks with ideal end-to-end distance $R_0 = bN^{1/2}$ (*black*). Neutral polymers in good solvent are self-avoiding walks with Flory end-to-end distance $R_F = bN^{0.588}$ (*red*). Polyelectrolytes with no salt adopt the highly extended directed random walk conformation (*blue*) with length L proportional to N

walk chain, making c^* proportional to $N^{-0.76}$. For polyelectrolytes without salt, we use the extended length $L \sim N$, making c^* proportional to N^{-2}. Figure 2 shows that the overlap concentration of neutral polymers in good solvent and of polyelectrolytes without salt shows reasonably well the expected power laws in molar mass. Neutral polymers in θ-solvent also exhibit nicely $c^* \sim N^{-1/2}$ (not shown). Quite generally,

$$R_{\mathrm{dilute}} \sim N^\nu \tag{1}$$

and

$$c^* \approx N/R_{\mathrm{dilute}}^3 \sim N^{1-3\nu} \tag{2}$$

with $\nu = 1/2$ for θ-solvent, $\nu = 0.588$ for good solvent, and $\nu = 1$ for polyelectrolytes without salt: the three universality classes for polymer solutions. Also shown in Fig. 2 are entanglement concentrations that will be discussed below. For neutral polymers in good solvent, Fig. 2 is qualitatively similar to previous estimations (Graessley 1980; Kulicke et al. 1991).

De Gennes showed that the correlation length, first introduced by Edwards (1966) is the key to understanding the structure of solutions above c^*, termed semidilute (Daoud et al. 1975; de Gennes 1979). To understand the correlation length ξ, we ask a simple question: How far away is the next chain? On scales smaller than ξ, there are mostly only monomers from the same chain and lots of solvent molecules; the chain adopts a local conformation similar to the dilute solution conformations of Fig. 1 (except for poor solvent), and dilute solution rules apply to both structure and dynamics inside ξ. On scales larger than ξ, there are many other chains, and the chain adopts a conformation that is a random walk of correlation blobs of size ξ, with melt-like rules applying for both structure and dynamics on large scales. Excluded volume interactions, hydrodynamic interactions and for polyelectrolytes also charge repulsion interactions, all get screened at the correlation length ξ, causing it to also be termed the screening length. Inside ξ, the different solutions have quite different chain conformations (Fig. 1), but the large-scale conformation of the chain in semidilute solution is always a random walk of correlation blobs, and dynamically, the chain behaves as though it were in a polymer melt.

In all solutions, de Gennes showed that the correlation length does not depend on chain length, and its concentration dependence can be inferred from a simple scaling argument:

$$\xi \approx R_{\mathrm{dilute}}(c/c^*)^y \sim c^{-\nu/(3\nu-1)} \tag{3}$$

where the last result was obtained requiring ξ to be independent of N (since at the scale of ξ, there is no information about how long the chain is) and using the N dependences of dilute size and overlap concentration from Eqs. 1 and 2. For θ-solvent, $\nu = 1/2$ and $\xi \sim c^{-1}$, for good solvent, $\nu = 0.588$ and $\xi \sim c^{-0.76}$, and for polyelectrolytes with no salt, $\nu = 1$ and $\xi \sim c^{-1/2}$. The end-to-end distance of the chain in semidilute solution is determined as a random walk of correlation blobs:

$$R \approx = \xi(N/g)^{1/2} \sim N^{1/2}c^{-(\nu-1/2)/(3\nu-1)} \tag{4}$$

where $g = c_n\xi^3$ is the number of monomers per correlation blob (c_n is the number density of monomers), making N/g the number of correlation blobs per chain. For θ-solvent, $\nu = 1/2$ and $R \sim N^{1/2}c^0$, so the ideal random walk persists at all concentrations. For good solvent, $\nu = 0.588$ and $R \sim N^{1/2}c^{-0.12}$, and for polyelectrolytes with no salt, $\nu = 1$ and $R \sim N^{1/2}c^{-1/4}$. All three of these power laws for coil size are well established experimentally (Daoud et al. 1975; Nierlich et al. 1985; Graessley 2003; Rubinstein and Colby 2003; Dobrynin and Rubinstein 2005, which constitutes strong evidence that de Gennes' ideas about solution structure and chain conformations are correct.

Osmotic pressure of semidilute solutions

Osmotic pressure is a colligative property—it counts the number density of species that contribute. In dilute solutions of neutral polymers, osmotic pressure is used to determine the number-average molar mass because it is essentially kT per solute molecule (the van't Hoff law; van't Hoff 1887). For neutral polymers in semidilute solutions, osmotic pressure directly counts the number density of correlation blobs (de Gennes 1979; Teraoka 2002; Graessley 2003; Rubinstein and Colby 2003)

$$\pi \approx kT/\xi^3 \sim c^{3\nu/(3\nu-1)} \tag{5}$$

and consequently is one of the two primary methods to determine the correlation length of semidilute solutions of neutral polymers. For θ-solvent, $\nu = 1/2$, $\xi \sim c^{-1}$ and $\pi \sim c^3$, while for good solvent, $\nu = 0.588$, $\xi \sim c^{-0.76}$ and $\pi \sim c^{2.31}$.

Polyelectrolyte solutions have significantly larger osmotic pressure than neutral polymer solutions. The membrane used to separate the polymer solution from the pure solvent has pores that are much larger than the small counterions of the polyelectrolyte. However, the Donnan equilibrium (Donnan and Guggenheim 1934;

Dobrynin et al. 1995) requires charge neutrality on both sides of the membrane owing to the large energies involved in separating charges macroscopic distances. Consequently, not only the polyelectrolyte but also all of its dissociated counterions contribute to the osmotic pressure. In the entire range of semidilute solutions where measurements of osmotic pressure have been reported (<10% polymer), there are many free counterions per correlation blob, and the osmotic pressure of such polyelectrolyte solutions with no salt is kT per free counterion

$$\pi \approx f c_n kT \tag{6}$$

where c_n is the number density of monomers and f is the fraction of those monomers bearing an effective charge (and hence, $f c_n$ is the number density of free counterions). Hence, for polyelectrolyte solutions without salt, osmotic pressure is a very important characterization tool to quantify the effective charge on the chain in solution, but tells nothing about the correlation length. The concentration dependence of osmotic pressure is shown in Fig. 3 for neutral polymer in θ-solvent (scaling as $\pi \sim c^3$), neutral polymer

Fig. 3 Comparison of the osmotic pressure of neutral polymer solutions (Flory and Daoust 1957) in θ-solvent: *black circles* $M_n = 90,000$ polyisobutylene in benzene at θ = 24.5°C, intermediate solvent: *open squares* $M_n = 90,000$ polyisobutylene in benzene at 50°C, good solvent: *red circles* $M_n = 90,000$ polyisobutylene in cyclohexane at 50°C; *red squares* $M_n = 90,000$ polyisobutylene in cyclohexane at 8°C) with the osmotic pressure of polyelectrolyte solutions with no added salt: *blue circles* $M_n = 320,000$ sodium poly(styrene sulfonate) in water at 25°C (Takahashi et al. 1970); *blue squares* high molar mass sodium poly(styrene sulfonate) in water at 25°C (Essafi et al. 2005). Clearly, solvent quality affects osmotic pressure of neutral polymer solutions, but the polyelectrolyte solutions have considerably larger osmotic pressure because there are many dissociated counterions in each correlation volume

in good solvent (scaling as $\pi \sim c^{2.31}$), neutral polymer in an intermediate solvent (also scaling as $\pi \sim c^{2.31}$), and a polyelectrolyte solution with no salt. The polyelectrolyte solution in water has orders of magnitude larger osmotic pressure than the neutral polymer solutions and roughly exhibits the $\pi \sim c$ scaling expected by Eq. 6. The data show progressively stronger deviations from Eq. 6 as concentration is raised, possibly the consequence of electrostatic interactions of counterions (Marcus 1955; Katchalsky 1971) or reflecting the fact that the dielectric constant of the solution increases with polymer concentration, perhaps causing more counterions to dissociate from the chain as concentration is raised (Oosawa 1971; Bordi et al. 2002, 2004).

Small-angle scattering

Small-angle scattering of neutrons (SANS) or X-rays (SAXS) are direct methods to probe the solution structure (Higgins and Benoit 1994; Pedersen and Schurtenberger 2004), and in contrast to osmotic pressure, scattering gives the correlation length of both neutral and polyelectrolyte semidilute solutions. The scattering function for neutral polymers in θ-solvent is of the Ornstein–Zernike form:

$$S(q) = \frac{S(0)}{1 + (q\xi)^2} \tag{7}$$

where q is the scattering wavevector. At low q, this function levels off at $S(0)$, while at high q, it decays as q^{-2}, as expected for a random walk chain inside the correlation length. For neutral polymers in good solvent, the scattering function is similar, but the high-q behavior reflects the fractal dimension of the self-avoiding walk inside the correlation length $\nu^{-1} = 0.588^{-1} = 1.7$,

$$S(q) = \frac{S(0)}{1 + (q\xi)^{1.7}} \tag{8}$$

making the scattering decay less rapidly than in θ-solvent for $q > \xi^{-1}$ (Rubinstein and Colby 2003, Section 5.7).

As might be anticipated from the scattering functions for neutral polymer solutions, the high-q form of the scattering function for polyelectrolyte solutions reflects the highly extended directed random walk conformation of the polyelectrolyte inside the correlation length, with fractal dimension 1 and $S(q) \sim q^{-1}$ for $q > \xi^{-1}$. However, polyelectrolyte solutions with no salt have a peak in their scattering function at $q = 2\pi\xi^{-1}$, and the scattering decays also as q is lowered. The scattering from neutral polymer solutions and polyelectrolyte

solutions are compared schematically in Fig. 4a. While thermal fluctuations can cause neutral polymer solutions to overlap their correlation volumes, such overlap is suppressed for polyelectrolyte solutions with no salt because that overlap would also require counterions to share the same volume. The enormous osmotic pressure of polyelectrolyte solutions caused by counterion entropy does not allow the correlation volumes to overlap, giving a peak in the scattering function (de Gennes et al. 1976; Dobrynin et al. 1995). Coupled with this counterion repulsion, the chains within their correlation volumes also are weakly repelled by their neighbors which tend to push the polyelectrolytes toward the correlation volume centers, shown schematically in Fig. 4b, making the peak in the scattering function at $q = 2\pi\xi^{-1}$ quite sharp for polyelectrolyte solutions with no salt.
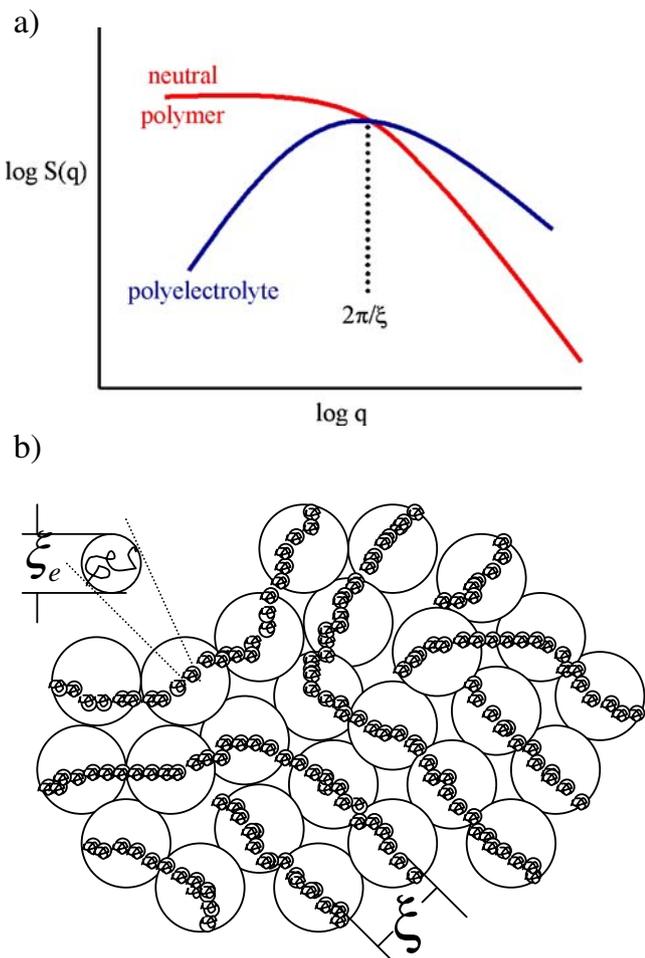
Fig. 4 a Schematic comparison of the structure factor from scattering of neutral polymer solutions (*red*) and polyelectrolyte solutions with no salt (*blue*). **b** Schematic structure of a semidilute polyelectrolyte solution with no salt (after Dou and Colby 2008)
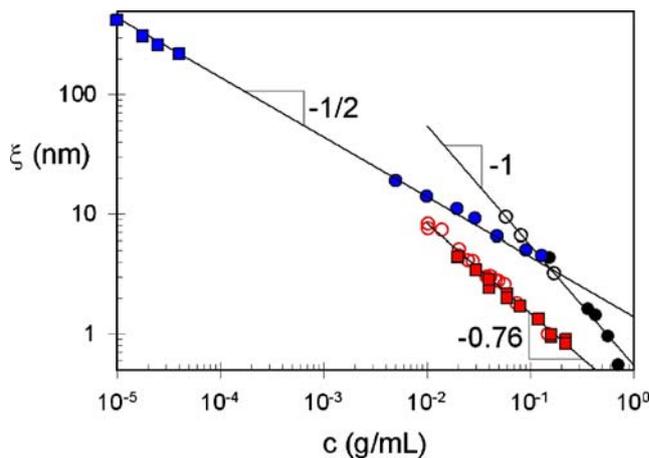
Fig. 5 Concentration dependence of correlation length of neutral and polyelectrolyte solutions: *blue squares* light scattering from sodium poly(styrene sulfonate) in water (Drifford and Dalbiez 1984); *blue circles* SANS from sodium poly(styrene sulfonate) in perdeuterated water (Nierlich et al. 1979); *red open circles* SANS from polystyrene in the good solvent carbon disulfide (Daoud et al. 1975); *red squares* SANS from polystyrene in the good solvent perdeuterated toluene (King et al. 1985); *black circles* (Geissler et al. 1990) and *black open circles* (Cotton et al. 1976) SANS from polystyrene in the θ-solvent perdeuterated cyclohexane at the θ-condition. *Lines* are the power laws predicted by de Gennes (Eq. 3)

The concentration dependence of the correlation length from scattering is shown in Fig. 5 for neutral polymer in θ-solvent (fit to Eq. 7 and scaling as $\xi \sim c^{-1}$), neutral polymer in good solvent (fit to Eq. 8 and scaling as $\xi \sim c^{-0.76}$), and a polyelectrolyte solution with no salt (taken as $2\pi/q_{max}$, scaling as $\xi \sim c^{-1/2}$). In all three cases, the de Gennes predicted power laws of Eq. 3 are observed, strongly supporting the notion that the structures of both neutral polymer solutions and polyelectrolyte solutions with no salt are well understood.

Entanglement concentration

At the time of writing his 1979 book, de Gennes assumed that chains would start to entangle at their overlap concentration c^* (de Gennes 1979). This assumption was perhaps influenced by the fact that there is only a subtle change in power law exponent for the concentration dependence of viscosity for neutral polymers in good solvent, in going from dilute to semidilute unentangled solution, as discussed below, and has caused the entanglement concentration to sometimes be confused with c^*. However, this assumption was quickly pointed out to be incorrect (Graessley 1980), and it is now well established that chain entanglement

occurs at concentrations significantly larger than c^*. In all three universality classes, there is an abrupt change (by roughly a factor of 3) in power law exponent for the concentration dependence of viscosity at the entanglement concentration c_e. Entanglement concentrations from such changes in the concentration dependence of viscosity are shown in Fig. 2 as circles for neutral polystyrene in the good solvent toluene (red circles) and for the sodium salt of sulfonated polystyrene in water with no salt (blue circles). Clearly, in both cases, $c_e > c^*$, meaning that there is a range of concentration that is semidilute where the chains are not entangled (Graessley 1980, 2008; Rubinstein and Colby 2003). Figure 2 shows that for neutral polymers in good solvent, $c_e \approx 10c^*$. For polyelectrolytes without salt, c_e seems to have a similar molar mass dependence as c_e and c^* of neutral polymers in good solvent, given by Eq. 2. Owing to the fact that polyelectrolyte solutions without salt have c^* proportional to N^{-2} (blue stars in Fig. 2), this observation means that solutions of high molar mass polyelectrolytes without salt have $c_e >> c^*$ (by more than a factor of 1,000 for the highest molar mass sulfonated polystyrene samples in Fig. 2; Boris and Colby 1998). For polyelectrolyte solutions in particular, the semidilute unentangled concentration regime, discussed below, is extremely important as it covers many decades of concentration.

Entanglement is also evident in the concentration dependence of recoverable compliance, seen in both poly(α-methyl styrene) solutions and polystyrene solutions in θ-solvents (Takahashi et al. 1991, Fig. 6) and for polybutadiene in an aromatic hydrocarbon (Graessley 2008, Fig. 8.6). However, systematic studies varying molar mass have not yet been done.

While our theoretical understanding of chain entanglement is unfortunately weak, simple existing models expect c_e to be larger than but proportional to c^* (Dobrynin et al. 1995; Rubinstein and Colby 2003; Dobrynin and Rubinstein 2005) for both neutral polymers in good solvent and polyelectrolytes with no salt. Figure 2 shows that this expectation is reasonably well observed for neutral polymers in good solvent, but clearly not observed for polyelectrolyte solutions with no salt. The case of neutral polymers in θ-solvent also violates this rule, but in that case, the violation is anticipated by theory, as discussed below.

Linear viscoelasticity of dilute solutions

In both dilute solution ($c < c^*$) and semidilute unentangled solution ($c^* < c < c_e$), there are no entanglement effects and the dynamics of all three universality classes

of polymers are described by simple bead-spring models, as pointed out by de Gennes (1976a, b, 1979). In dilute solutions of neutral polymers, hydrodynamic interactions dominate within the pervaded volume of the coil and the Zimm model describes linear viscoelasticity (Zimm 1956; Doi and Edwards 1986; Rubinstein and Colby 2003; Graessley 2008). In semidilute unentangled solutions of both neutral polymers and polyelectrolytes with no salt, excluded volume and any charge repulsion are screened beyond the correlation length, so the chain is a random walk on its largest scales and the hydrodynamic interactions are screened beyond the correlation length. Inside the correlation blobs, hydrodynamic interactions are important and the Zimm model describes linear viscoelastic response, while on larger scales (and longer times), the Rouse model describes linear viscoelasticity (Rouse 1953; Doi and Edwards 1986; Rubinstein and Colby 2003; Graessley 2008). Doi and Edwards (1986) showed that the currently accepted solutions of these two models (exact for the Rouse model; approximate for the Zimm model) have identical forms for the stress relaxation modulus when cast in terms of the sum of N exponential relaxation modes

$$G(t) = \frac{cRT}{M} \sum_{p=1}^{N} \exp(-t/\tau_p) \qquad (9)$$

where R is the gas constant, c is the mass concentration of polymer, p is the mode index, and the τ_p are the mode relaxation times. The pre-summation factor in Eq. 9 for both the Rouse and Zimm models is simply kT per chain, sometimes written as $c_n kT/N$, where c_n is the monomer number density, making c_n/N the number density of chains in solution. The differences in the models lie in the forms of the predicted mode relaxation times or mode structure.

In dilute solution, the Zimm model applies to the entire chain, which relaxes (adopts a new conformation) as a hydrodynamically coupled object with longest relaxation time

$$\tau_Z = \frac{1}{2\sqrt{3\pi}} \frac{\eta_s R_{dilute}^3}{kT} \approx \tau_0 N^{3v} \qquad (10)$$

where η_s is the solvent viscosity, R_{dilute} is the dilute solution size of the chain, and τ_0 is the relaxation time of a Kuhn monomer, corresponding to the shortest time in the bead-spring models with mode index $p = N$. Mode index p refers to sections of the chain having N/p monomers, and these sections relax as entire chains of N/p monomers relax, with relaxation time

$$\tau_p = \tau_0 \left(\frac{N}{p}\right)^{3v} = \frac{\tau_z}{p^{3v}} \qquad (11)$$

where τ_Z is the longest Zimm time, corresponding to relaxation of the entire dilute solution chain having full hydrodynamic coupling, with mode index $p = 1$. Equations 9–11 predict fully the linear viscoelasticity of dilute solutions of neutral polymers in both good solvent (where R_{dilute} is the Flory end-to-end distance $R_{\text{F}} = bN^{0.588}$ of the self-avoiding walk chain) and θ-solvent (where R_{dilute} is the ideal coil end-to-end distance $R_0 = bN^{1/2}$).

In an unentangled melt of short polymer chains, the Rouse model applies to the entire chain and hydrodynamic interactions are fully screened with longest relaxation time

$$\tau_R = \frac{\zeta N R^2}{6\pi^2 kT} = \frac{\zeta b^2 N^2}{6\pi^2 kT} \approx \tau_0 N^2 \qquad (12)$$

where ζ is the Kuhn monomer friction coefficient, and the final result made use of random walk statistics in the melt $R = bN^{1/2}$. Again, the mode index p refers to sections of the chain having N/p monomers, and these sections relax as entire chains of N/p monomers relax, with relaxation time

$$\tau_p = \tau_0 \left(\frac{N}{p}\right)^2 = \frac{\tau_R}{p^2} \qquad (13)$$

where again τ_0 is the relaxation time of a Kuhn monomer, corresponding to the shortest mode with index $p = N$, and τ_R is the longest Rouse time, corresponding to relaxation of the entire unentangled chain without hydrodynamic interactions, with mode index $p = 1$. Equations 9, 12, and 13 predict fully the linear viscoelasticity of polymer melts with chains too short to be entangled.

Rubinstein and Colby (2003) showed that Eqs. 9–13 for the pure Zimm and pure Rouse models can be replaced with an approximate form for the stress relaxation modulus that is the product of a power law and an exponential cutoff

$$G(t) = c_n kT \left(\frac{t}{\tau_0}\right)^{-1/\mu} \exp(-t/\tau) \text{ for } t > \tau_0 \qquad (14)$$

where c_n is the monomer number density, making the prefactor kT per monomer, τ is the longest relaxation time (i.e., either τ_R for the Rouse model or τ_Z for the Zimm model), and following Doi and Edwards (1986), μ is the exponent for the reciprocal p dependence of the mode relaxation times in Eqs. 11 and 13 (i.e., $\mu = 2$ for the Rouse model and $\mu = 3\nu$ for the Zimm model, giving $\mu = 3/2$ in dilute θ-solvent and $\mu = 1.76$ in good solvent). Equation 14 is a remarkably good approximation for both the Rouse and Zimm models (Rubinstein and Colby 2003) and is far more convenient than Eqs. 9–13. Either Eq. 9 or Eq. 14 can be

easily transformed to the frequency domain yielding analytical expressions for the frequency dependence of the storage modulus G' and loss modulus G''. Given the form of Eq. 14 as the product of a power law and an exponential cutoff, it is hardly surprising that the frequency dependence of G' and G'' at high frequencies is a power law in both the Rouse and Zimm models

$$G' \sim G'' \sim \omega^{1/\mu} \text{ for } 1/\tau << \omega << 1/\tau_0 \qquad (15)$$

while $G' \sim \omega^2$ and $G'' \sim \omega$ in the limit of low frequencies, as for any viscoelastic liquid. For both the pure Rouse and pure Zimm models, the reduced moduli (Doi and Edwards 1986) are predicted to be universal when plotted against $\omega\tau$, where τ is the longest relaxation time.

Owing to the remarkable devices developed by Ferry, Schrag and coworkers (Ferry 1980), linear viscoelastic data actually have been measured in dilute solutions of long chain linear polymers. Figure 6 shows the reduced moduli plotted against $\omega\tau_Z$, for dilute polystyrene solutions in two θ-solvents (Johnson et al. 1970), measured using a multiple-lumped resonator. The reduced storage modulus is G' divided by the kT per chain pre-summation factor of Eq. 9, cRT/M. The reduced loss modulus first subtracts off $\omega\eta_s$ (to focus on the polymer contribution) and then is divided by cRT/M. The curves in Fig. 6 are the universal predictions of the Zimm model for the oscillatory shear response of any neutral linear polymer in dilute solution in any θ-solvent. Dilute solution data for different
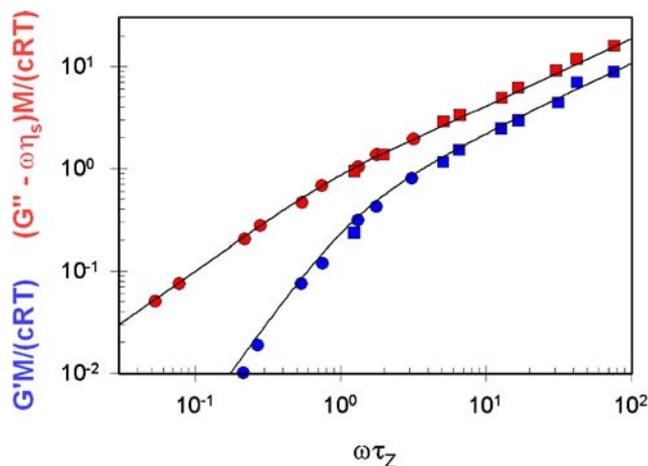
Fig. 6 Linear viscoelastic response expressed in terms of reduced moduli for dilute $M = 860{,}000$ polystyrene solutions in two θ-solvents (Johnson et al. 1970). *Red* are reduced loss moduli, *blue* are reduced storage moduli, *circles* are in decalin at 16°C, *squares* are in di-2-ethylhexylphthalate at 22°C. *Curves* are predictions of the Zimm model with Flory exponent $\nu = 1/2$ (following Rubinstein and Colby 2003, Fig. 8.7)

molar mass polymers, different linear polymer types, different concentrations, and different θ-solvents are all predicted to also fall on these curves. Figure 6 is convincing evidence that the Zimm model really describes completely the linear viscoelastic response of dilute neutral polymers in θ-solvent. The experimental situation is unfortunately a bit more complicated in dilute solutions of neutral polymers in good solvents as the excluded volume that swells the chain in good solvent apparently weakens the hydrodynamic interaction (Hair and Amis 1989; Graessley 2008), and the details of this have not yet caught the attention of theorists. A very similar situation is seen for dilute solutions of sulfonated polystyrene with excess salt (Rosser et al. 1978) as expected since polyelectrolytes with excess salt (more salt ions than free counterions) are in the same universality class as neutral polymers in good solvent, owing to the similarity of screened excluded volume interactions and screened electrostatic interactions (Pfeuty 1978; Dobrynin et al. 1995).

The pure Rouse model applies to melts of linear polymers that are too short to be entangled. Figure 7 shows the reduced moduli plotted against $\omega\tau_R$ for short linear polystyrene chains at a reference temperature of 160°C (Onogi et al. 1970). The reduced storage and loss moduli are divided by the kT per chain pre-summation factor of Eq. 9, $\rho RT/M$, where ρ is the mass density. The shortest chains studied ($M_w = 8900$, large circles in Fig. 7) are significantly below the entanglement molar mass of polystyrene ($M_e = 17,000$), and those
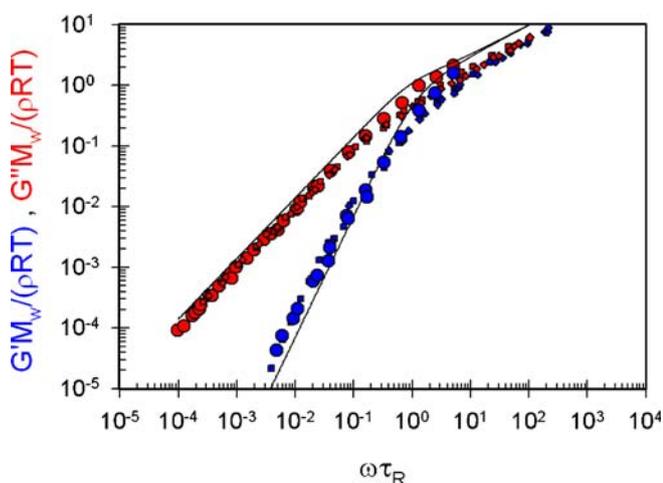
data agree nicely with the Rouse predictions, but the temperature was not low enough to observe the predicted slope of 1/2. The two higher molar mass samples are close to ($M_w = 14800$, small squares in Fig. 7) and larger than ($M_w = 28900$, small diamonds in Fig. 7) the entanglement molar mass. While these datasets do show the expected slope of 1/2 at high frequencies, the data are below the Rouse predictions, presumably due to a mild effect of interchain entanglements.

Linear viscoelasticity of semidilute unentangled solutions

Given the success of the pure Zimm model in dilute θ-solvents (Fig. 6) and the pure Rouse model in unentangled melts (Fig. 7), one would expect semidilute unentangled solutions to be easily described. De Gennes' instruction for semidilute solutions (de Gennes 1979) is to simply use dilute solution rules on scales inside the correlation length and melt rules on larger scales where the entire chain relaxes. As described in detail in my textbook (Rubinstein and Colby 2003, Section 8.5), the modes inside the correlation length should relax by the Zimm model, up to the relaxation time of the correlation volume

$$\tau_\xi \approx \frac{\eta_s}{kT}\xi^3 \tag{16}$$

and the random walk chain of correlation blobs should relax by the Rouse model with terminal relaxation time

$$\tau_{\text{chain}} \approx \tau_\xi \left(\frac{N}{g}\right)^2 \approx \frac{\eta_s N}{c_n kT}\left(\frac{R}{\xi}\right)^2 \tag{17}$$

where $g = c_n\xi^3$ is the number of Kuhn monomers per correlation blob and N/g is the number of correlation blobs per chain. For linear viscoelastic response, a slope of 1/2 is expected at intermediate frequencies (where the Rouse chain of correlation blobs is relaxing) and a higher slope at high frequencies ($1/\mu = 2/3$ in dilute θ-solvent and $1/\mu = 0.57$ in good solvent; see Fig. 8.10 of Rubinstein and Colby 2003).

Figure 8 shows G' and G'' calculated from oscillatory flow birefringence (OFB) data for a semidilute unentangled poly(α-methyl styrene) solution with $c = 0.105$ g/cm^3 in the polychlorinated biphenyl solvent Arochlor at 25°C (Lodge and Schrag 1982). This solution has roughly 20 Kuhn monomers per correlation volume, and each chain with $M = 400,000$ has roughly $N/g \approx 40$ correlation blobs per chain. Hence, we expect and observe roughly three decades of Rouse slope of 1/2 in Fig. 8. Unfortunately, at higher frequencies, the transformation of oscillatory flow birefringence

Fig. 7 Linear viscoelastic response expressed in terms of reduced moduli for low molar mass narrow distribution polystyrene melts at 160°C (Onogi et al. 1970). *Red* are reduced loss moduli, *blue* are reduced storage moduli, *large circles* are $M_w = 8,900$, *small squares* are $M_w = 14,800$, *small diamonds* are $M_w = 28900$. *Curves* are predictions of the Rouse model (following Graessley 2008, Fig. 6.19a)
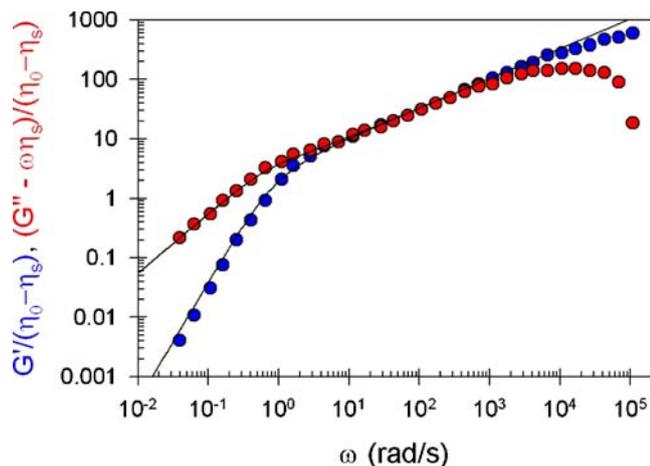
Fig. 8 Linear viscoelastic response from oscillatory flow birefringence studies of a semidilute unentangled $M = 400{,}000$ poly(α-methyl styrene) solution ($c = 0.105$ g/cm^3) in Arochlor at 25°C (Lodge and Schrag 1982). *Red* are reduced loss moduli, *blue* are reduced storage moduli, *curves* are predictions of the Rouse model. The roll-off of loss moduli at high frequencies indicates the transformation from OFB to G' and G'' fails at high frequencies

data to G' and G'' apparently fails (Lodge and Schrag 1982), so these data cannot be used to see whether the Zimm predictions hold inside the correlation blobs. Many similar examples can be found in the PhD theses from Schrag's group.

Figure 9 shows G' and G'' measured by the multiple-lumped resonator for semidilute unentangled quaternized poly(2-vinyl pyridine) chloride solutions in
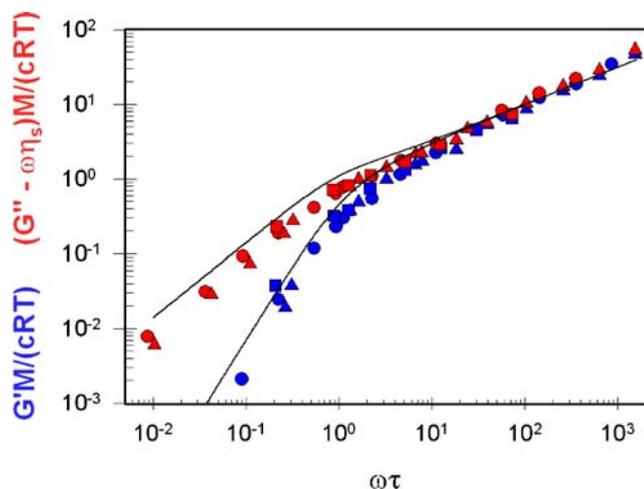
Fig. 9 Linear viscoelastic response from multiple lumped resonator studies of semidilute unentangled quaternized poly(2-vinyl pyridine) chloride solutions in 0.0023 M HCl/water at 25°C (Hodgson and Amis 1991). *Red* are reduced loss moduli, *blue* are reduced storage moduli, *squares* are $c = 0.5$ g/L, *triangles* are $c = 1.0$ g/L, *circles* are $c = 2.0$ g/L. *Curves* are predictions of the Rouse model (following Rubinstein and Colby 2003, Fig. 8.5)

0.0023 M HCl/water at 25°C (Hodgson and Amis 1991). Data for three different concentrations are reduced nicely for these semidilute unentangled polyelectrolyte solutions without added salt and agree well with the predictions of the Rouse model, shown as solid curves. Very similar data were reported for three molar masses of sodium poly(styrene sulfonate) in water at significantly higher concentrations but still in the semidilute unentangled regime using conventional oscillatory shear rheometry (Takahashi et al. 1996).

The data in Figs. 8 and 9 (and elsewhere) present strong evidence that the Rouse model does indeed describe the linear viscoelastic response of polymers in semidilute unentangled solution. More commonly, the terminal dynamics of polymers have been measured and reported as either terminal relaxation time, viscosity, or diffusion coefficient. The predictions for terminal dynamics of semidilute unentangled solutions are summarized in Table 1, based on Eqs. 3, 4, and 17, for the three universality classes. Diffusion coefficients provide the strongest evidence for the Rouse scaling of terminal dynamics of neutral polymers in semidilute unentangled good solvent (Rubinstein and Colby 2003, Fig. 8.9) with the expected decade in concentration where $D \sim c^{-0.54}$ between c^* and c_e clearly observed. There is almost no evidence for semidilute unentangled θ-solvent probably because for high molar mass chains, there is significantly less than one decade of semidilute unentangled solution for neutral polymers in θ-solvent, as discussed in the next section.

A number of the predictions in Table 1 for polyelectrolyte solutions with no salt are unusual and deserve discussion. Firstly, the terminal relaxation time has a negative exponent for its concentration dependence. This means that polyelectrolyte solutions are predicted to be *rheologically unique* as they are the only material known that has longest relaxation time *increase* on dilution! The physics for this prediction is quite simple: The Rouse model always predicts $\tau_{\text{chain}} \sim NR^2/(\xi^2 c)$, as shown in Eq. 17. For polyelectrolyte solutions, $\xi \sim c^{-1/2}$, so the denominator $\xi^2 c$ is independent of c, leaving $\tau_{\text{chaim}} \sim NR^2$ (a common Rouse result). As concentration is raised, polyelectrolyte solutions have their chain size decrease rapidly (Eq. 4 with $\nu = 1$ predicts $R \sim c^{-1/4}$), making the relaxation time decrease as $\tau_{\text{chain}} \sim N^2 c^{-1/2}$. This prediction was first observed for sodium poly(styrene sulfonate) in 95% glycerol/5% water with no added salt (Zebrowski and Fuller 1985). Since then, this unique prediction has been tested often for sodium poly(styrene sulfonate) in water (Boris and Colby 1998; Chen and Archer 1999), sodium poly(2-acrylamido-2-methylpropane sulfonate) in water (Krause et al. 1999), partially quaternized

Table 1 De Gennes scaling predictions of solution structure and Rouse model predictions for terminal polymer dynamics in semidilute unentangled solutions for the three universality classes

	General equation	Neutral in θ-solvent	Neutral in good solvent	Polyelectrolyte with no salt
Scaling exponent	$v \equiv \partial(\log R_{\text{dilute}})/\partial(\log N)$	$v = 1/2$	$v = 0.588$	$v = 1$
Correlation blob size	$\xi \sim N^0 c^{-v/(3v-1)}$	$\xi \sim N^0 c^{-1}$	$\xi \sim N^0 c^{-0.76}$	$\xi \sim N^0 c^{-1/2}$
Polymer size	$R \sim N^{1/2} c^{-(v-1/2)/(3v-1)}$	$R \sim N^{1/2} c^0$	$R \sim N^{1/2} c^{-0.12}$	$R \sim N^{1/2} c^{-1/4}$
Chain relaxation time	$\tau_{\text{chain}} \sim N^2 c^{(2-3v)/(3v-1)}$	$\tau_{\text{chain}} \sim N^2 c$	$\tau_{\text{chain}} \sim N^2 c^{0.31}$	$\tau_{\text{chain}} \sim N^2 c^{-1/2}$
Terminal modulus	$G = N^{-1} c_n kT$	$G = N^{-1} c_n kT$	$G = N^{-1} c_n kT$	$G = N^{-1} c_n kT$
Polymer contribution to viscosity	$\eta - \eta_s \approx G\tau_{\text{chain}} \sim Nc^{1/(3v-1)}$	$\eta - \eta_s \sim Nc^2$	$\eta - \eta_s \sim Nc^{1.3}$	$\eta - \eta_s \sim Nc^{1/2}$
Diffusion coefficient	$D \approx R^2/\tau_{\text{chain}} \sim N^{-1} c^{-(1-v)/(3v-1)}$	$D \sim N^{-1} c^{-1}$	$D \sim N^{-1} c^{-0.54}$	$D \sim N^{-1} c^0$

poly(2-vinyl pyridine) chloride in ethylene glycol (Dou and Colby 2006), and partially quaternized poly(2-vinyl pyridine) iodide in *N*-methyl formamide (Dou and Colby 2008).

The fact that relaxation time of semidilute unentangled polyelectrolyte solutions increases as concentration is lowered, reaching a largest value at the overlap concentration c^*, means that shear thinning starts at progressively lower rates as the solution is diluted (Colby et al. 2007). This complicates much of the early rheology literature on polyelectrolyte solutions because this strong shear thinning was not recognized (see Boris and Colby 1998, Fig. 10). Many reports were made for viscosity using gravity-driven capillary viscometers (as the viscosity of semidilute unentangled solutions is never more than 300 times that of the solvent) which have shear thinning effects for polyelectrolyte solutions with *M* larger than about 200,000.

Since the terminal modulus of the Rouse model is always $c_n kT/N$ (see Table 1), the unusual concentration dependence of relaxation time leads to an unusually weak concentration dependence of specific viscosity $\eta_{\text{sp}} \equiv (\eta - \eta_s)/\eta_s \sim Nc^{1/2}$ for polyelectrolyte solutions with no salt, known as the Fuoss Law (Fuoss and Strauss 1948; Fuoss 1948, 1951). Since Fuoss' work, this scaling has been observed for sodium polyphosphate in water (Strauss and Smith 1953), potassium cellulose sulfate and potassium polyacrylate in water (Terayama and Wall 1955), sodium poly(styrene sulfonate) in water (Fernandez Prini and Lagos 1964; Cohen et al. 1988; Boris and Colby 1998), sulfonated polystyrene with a variety of counterions in a variety of polar solvents, in particular dimethyl sulfoxide (Agarwal et al. 1987), sodium partially sulfonated polystyrene in dimethyl formamide (Kim and Peiffer 1988; Hara et al. 1988), a quaternary ammonium chloride polymer in a variety of polar solvents (Jousset et al. 1998), sodium poly(2-acrylamido-2-methylpropane sulfonate) in water (Krause et al. 1999; Dragan et al. 2003), partially quaternized poly(2-vinyl pyridine) chloride in ethylene

glycol (Dou and Colby 2006), and partially quaternized poly(2-vinyl pyridine) iodide in *N*-methyl formamide (Dou and Colby 2008). Figure 10 compares the concentration dependences of specific viscosity for two polymers with $N = 3{,}230$ monomers: neutral poly(2-vinyl pyridine) in the good solvent ethylene glycol (red) with 55% quaternized poly(2-vinyl pyridine) chloride polyelectrolyte in ethylene glycol (blue; Dou and Colby 2006). Both have $\eta_{\text{sp}} \sim c$ in dilute solution, as expected by the Zimm model. The polyelectrolyte has much lower overlap concentration because charge repulsion stretches the dilute chains. In semidilute unentangled solution, the polyelectrolyte has higher viscosity with
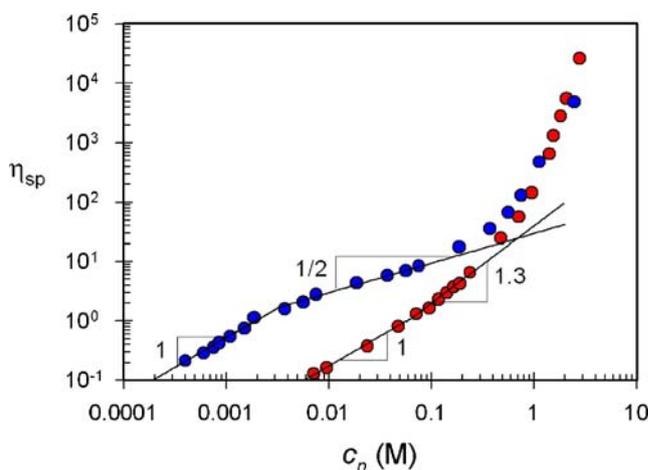
Fig. 10 Comparison of specific viscosity in the good solvent ethylene glycol of a neutral polymer (poly(2-vinyl pyridine), *red*) and the same polymer that has been 55% quaternized (poly(2-vinyl pyridine) chloride, *blue*; Dou and Colby 2006) plotted as functions of the number density of monomers with units of moles of monomer per liter. Slopes of unity for $\eta_{\text{sp}} < 1$ are expected by the Zimm model in dilute solution ($c < c^*$). Slopes of 1/2 and 1.3 for $1 < \eta_{\text{sp}} < 20$ are expected by the Rouse model for semidilute unentangled solutions of polyelectrolytes and neutral polymers, respectively. At higher concentrations, entangled solution viscosity data are shown that are consistent with the $3\times$ larger slopes predicted for entangled solutions

$\eta_{sp} \sim c^{1/2}$ (Fuoss Law), while the neutral polymer in good solvent has $\eta_{sp} \sim c^{1.3}$, and both results are predicted by the Rouse model for semidilute unentangled solutions (see Table 1). Both types of polymer have $\eta_{sp} \approx 1$ at c^*, meaning that the solution viscosity is roughly twice the solvent viscosity at c^*. Equation 2 based on dilute end-to-end distance for neutral polymers in good solvent always gives a similar value of c^* as that based on viscosity, but many experimentalists use Eq. 2 based on radius of gyration, which gives a c^* that is roughly a factor of 10 higher (i.e., near c_e for neutral polymers in good solvent). Coupled with the fact that de Gennes' book (de Gennes 1979) suggests that entanglement starts at c^* means that many workers have confused c_e with c^*. Operationally, a very simple measurement of viscosity at c^* can reveal whether it is c^* or c_e: The viscosity at c^* is always of order twice the solvent viscosity, while the viscosity at c_e is 10 to 300 times the solvent viscosity (and consequently cannot possibly be c^* as there is no way for dilute solutions to have such high viscosity!).

The diffusion coefficient of semidilute unentangled polyelectrolyte solutions with no salt also has an unusual concentration dependence; D is independent of concentration (see Table 1). This result has not been as extensively tested as viscosity or relaxation time, but some data for sodium poly(styrene sulfonate) in water with no added salt do show this predicted scaling (Oostwal et al. 1993), as will be shown later in Fig. 15b.

There is firm evidence that for neutral polymers in good solvent, there is a semidilute unentangled concentration regime that is roughly one decade in concentration ($c_e \approx 10c^*$, compare red stars and red circles in Fig. 2, see also Fig. 2 of Takahashi et al. 1992) and that the Rouse model describes linear viscoelasticity (see Fig. 8). For polyelectrolyte solutions with no salt, the semidilute unentangled regime of concentration covers a considerably wider range (compare blue stars and blue circles in Fig. 2), and again, the Rouse model describes linear viscoelasticity (see Fig. 9). Particularly for high molar mass polyelectrolytes in very polar solvents like water, $c_e > 1,000c^*$, allowing the predicted Rouse concentration dependences of relaxation time, viscosity, and diffusion coefficient to be observed clearly. For processing operations such as high-speed coating that require the solution to not have too much elastic character, unentangled semidilute solutions are extremely important. Owing to environmental concerns, we expect coatings from aqueous solutions of semidilute unentangled polyelectrolytes to play an important role in industry in the near future, most likely with surfactant added to control surface tension (Plucktaveesak et al. 2003).

Linear viscoelasticity of entangled solutions

To understand entanglement effects in polymer solutions, it is necessary to introduce another length scale that is not observable in experiments probing static structure of the solution. This dynamic length scale is the Edwards tube diameter a. It is crucial at the outset to recognize that this tube diameter (or entanglement spacing) is significantly larger than the correlation length (or spacing between chains). Neighboring chains restrict the lateral excursions of a chain to an entropic nearly parabolic potential (Rubinstein and Colby 2003, Fig. 7.10) and when the lateral excursion raises the potential by kT, this defines the effective diameter of the confining tube. Neutron spin echo (NSE) has been used to observe the lateral excursions directly by fitting the dynamic structure factor $S(q,t)$ to the tube model predictions to "measure" the tube diameter (Higgins and Roots 1985). This method has been extensively applied to polymer melts by Richter and coworkers and the current situation was recently summarized (Graessley 2008, Table 7.2). NSE has also been applied to solutions of hydrogenated polybutadiene (PEB-2, indicating that the starting polybutadiene had only 2% vinyl incorporation) in low molar mass alkanes which are good solvents (Richter et al. 1993).

Since the tube diameter is larger than the correlation length, the entanglement strand in any solution is a random walk of correlation blobs. In analogy with rubber elasticity (Ferry 1980; Rubinstein and Colby 2003), the terminal (or plateau) modulus is the number density of entanglement strand times kT (i.e., kT per entanglement strand). The correlation blobs are space-filling ($c_n = g/\xi^3$) and the volume of an entanglement strand is $\xi^3 N/g = \xi^3 (a/\xi)^2 = a^2\xi$, making the terminal modulus (Colby and Rubinstein 1990)

$$G_e = \frac{kT}{a^2\xi} \tag{18}$$

which allows the tube diameter to be calculated from measured values of G_e and ξ. Concentration dependences of correlation length and tube diameter are compared in Fig. 11 for neutral polymers in good solvent (red), neutral polymers in θ-solvent (black), and polyelectrolyte solutions with no added salt (blue). The lower lines in Fig. 11 are fits to Eq. 3 using the expected slopes for neutral polymers in θ-solvent ($\nu = 1/2$ and $-\nu/(3\nu - 1) = -1$), for neutral polymers in good solvent ($\nu = 0.588$ and $-\nu/(3\nu - 1) = -0.76$), and for polyelectrolyte solutions with no salt ($\nu = 1$ and $-\nu/(3\nu - 1) = -1/2$) consistent with Fig. 5. The limited data on tube diameter
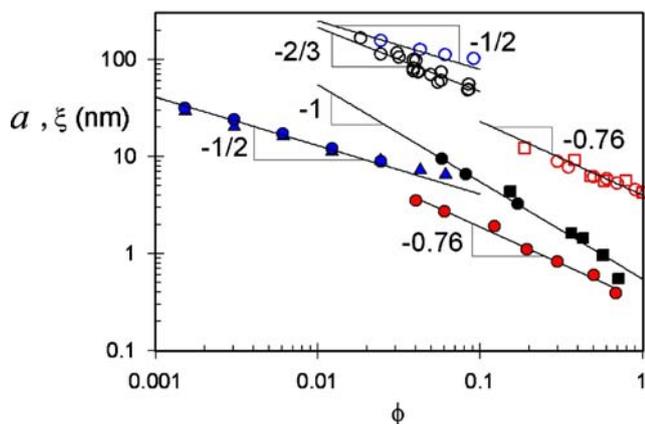
Fig. 11 Comparison of the concentration dependence of correlation length (*filled symbols*) and tube diameter (*open symbols*) for neutral polymers in good solvent (*red*, hydrogenated polybutadienes (*hPB*) in linear alkanes) with neutral polymers in θ-solvent (*black*, polystyrene (*PS*) in cyclohexane at the θ-temperature) and with polyelectrolyte solutions with no salt (*blue*, partially quaternized poly(2-vinyl pyridine) iodide (*QP2VP-I*) in *N*-methyl formamide (*NMF*)). *Filled red circles* are correlation length from SANS (Tao et al. 1999), *open red circles* are tube diameter calculated using Eq. 18 from the measured terminal loss modulus peak for PEB-7 (Tao et al. 1999), and *open red squares* are tube diameter calculated from fitting NSE data on PEB-2 to the Ronca model (Richter et al. 1993). *Filled black squares* (Geissler et al. 1990) and *filled black circles* (Cotton et al. 1976) are correlation length from SANS, *open black circles* are tube diameter calculated using Eq. 18 from the measured terminal modulus (Adam and Delsanti 1984). *Filled blue triangles* are correlation length from SAXS, *filled blue circles* are correlation length calculated from specific viscosity of semidilute unentangled solutions, *four open blue circles* are tube diameter calculated using Eq. 18 from the measured terminal modulus of the four entangled solutions (Dou and Colby 2008). It is worth noting that Tao et al. (1999) estimated tube diameter a different way (not using Eq. 18), and those results do not agree well with Richter et al. (1993). *Lower lines* are Eq. 3 with $\nu = 0.588$ for good solvent ($\xi = 0.33$ nm$\phi^{-0.76}$ for hPB in linear alkanes), $\nu = 1/2$ for θ-solvent ($\xi = 0.55$ nmϕ^{-1} for PS in cyclohexane), and $\nu = 1$ for polyelectrolytes ($\xi = 1.3$ nm$\phi^{-1/2}$ for QP2VP-I in NMF). *Upper lines* are expected power laws for the tube diameter (Table 2) with $a = 4$ nm$\phi^{-0.76}$ for hPB in alkanes (good solvent), $a = 10$ nm$\phi^{-2/3}$ for PS in the θ-solvent cyclohexane, and $a = 25$ nm$\phi^{-1/2}$ for QP2VP-I in NMF (those data are better fit by $a = 50$ nm$\phi^{-1/3}$, consistent with the unexpected N-dependence of entanglement concentration in Fig. 2, showing that scaling fails for polyelectrolyte entanglement)

for neutral polymers in good solvent and for polyelectrolyte solutions with no added salt seem to indicate that the tube diameter is proportional to but larger than the correlation length. For the neutral polymer hydrogenated polybutadiene in various linear alkanes (good solvents), $a \approx 10\xi$, and for the polyelectrolyte solutions of partially quaternized poly(2-vinyl pyridine) in *N*-methyl formamide with no added salt, $a \approx 20\xi$. In contrast, for neutral polystyrene in the θ-solvent cyclohexane, the tube diameter has a weaker concen-

tration dependence than the correlation length. This result is also anticipated by a two-parameter scaling theory (Colby and Rubinstein 1990) which predicts that while $\xi \sim c^{-1}$, reflecting the distance between ternary contacts acting on osmotic pressure, $a \sim c^{-2/3}$, reflecting the distance between binary contacts whose effect on osmotic pressure cancels out at the θ-temperature, but are controlling entanglement and plateau modulus. Using the concentration-dependent length scales in Eq. 18 leads directly to predictions of the concentration dependence of plateau modulus in entangled solutions for all three universality classes.

$$G_e = \frac{kT}{a^2\xi} \sim \begin{cases} c^{7/3} & \text{for θ-solvent} \\ c^{2.31} & \text{for good solvent.} \\ c^{3/2} & \text{for polyelectrolyte} \end{cases} \tag{19}$$

Figure 12 shows that these predicted concentration dependences are indeed observed in experiments for neutral polymers in either good solvent or θ-solvent. The
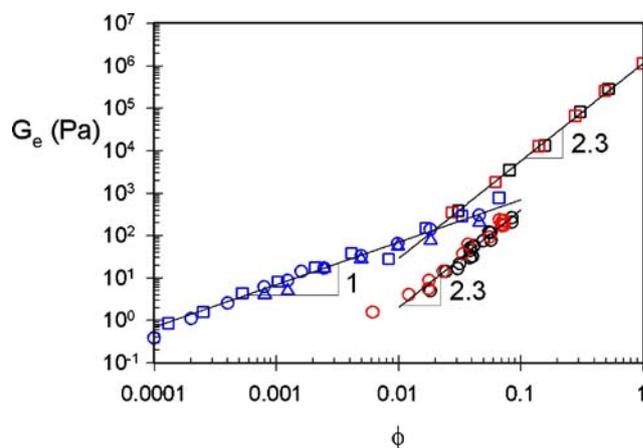
Fig. 12 Comparison of the concentration dependence of terminal modulus for neutral polymers in good solvent: *red circles* are $G_e = \eta/\tau$ for polystyrene in benzene (Adam and Delsanti 1983); *red squares* are plateau modulus estimated from oscillatory shear for polybutadiene in phenyloctane (Colby et al. 1991), with neutral polymers in θ-solvent: *black circles* are $G_e = \eta/\tau$ for polystyrene in cyclohexane at the θ-temperature (Adam and Delsanti 1984); *black squares* are plateau modulus estimated from oscillatory shear for polybutadiene in dioctyl phthalate (Colby et al. 1991) and with polyelectrolyte solutions with no added salt: *blue circles* are $G_e = \eta/\tau$ with τ from the onset of shear thinning in steady shear; *blue triangles* are $G_e = \eta/\tau$ with τ from oscillatory shear both for $M = 1.7 \times 10^6$ sodium poly(2-acrylamido-2-methylpropane sulfonate) in water; *blue squares* are $G_e = \eta/\tau$ with τ from the onset of shear thinning in steady shear for $M = 9.5 \times 10^5$ sodium poly(2-acrylamido-2-methylpropane sulfonate) in water (Krause et al. 1999). For the neutral polymer solutions, the lines have slopes of 2.3 expected by Eq. 19 for entangled solutions. For the polyelectrolyte solutions, the line has the slope of unity and is numerically slightly smaller than kT per chain, expected for unentangled semidilute solutions

polybutadiene solutions have plateau modulus from oscillatory shear (Colby et al. 1991), with data that extend all the way to the melt, as this polymer has glass transition temperature of −99°C, and Eq. 19 applies for the entire measured range ($0.02 < \phi \leq 1$). The polystyrene solutions necessarily cover a more limited range, and the 2.3 slope expected for both good solvent and θ-solvent in Eq. 19 applies well in the range ($0.01 < \phi < 0.1$). For the polystyrene solutions, viscosity and longest relaxation time were measured and the terminal modulus was calculated as $G_e = \eta/\tau$ (Adam and Delsanti 1983, 1984). In both sets of data for the neutral polymer solutions, good solvent and θ-solvent have indistinguishable concentration dependences of plateau modulus, as expected by Eq. 19. Another important point arises from the neutral polymer solution data in Fig. 12. Many polymers have glass transition temperature significantly above ambient and have the limitation shown for polystyrene, not exceeding about 10% polymer. A variety of exponents between 2 and 2.5 have been reported in the literature for the concentration dependence of plateau modulus (see Pearson 1987 for a review), but these studies usually cover less than a decade of concentration and are all consistent with a slope of 2.3 if the power law is forced to go through the known plateau modulus of the polymer melt. The polybutadiene data in Fig. 12 cover the entire range and certainly suggest that a single value of the exponent is appropriate.

The terminal modulus is estimated for the polyelectrolyte solutions in a similar way as Adam and Delsanti used for polystyrene solutions, from measured viscosity and terminal relaxation time as $G_e = \eta/\tau$, with τ either determined as the reciprocal of the shear rate where shear thinning starts or as the terminal response in oscillatory shear (Fig. 12 shows these two methods agree nicely). Most of the polyelectrolyte solution data in Fig. 12 correspond to semidilute unentangled solution where the Rouse model expects the modulus is $c_n kT/N$ (kT per chain), as observed. However, the highest decade of concentration for the $M = 1.7 \times 10^6$ sample (blue circles and blue triangles in Fig. 12) have $c > c_e$ and should show the 3/2 slope of Eq. 19, but do not.

Analogous to semidilute unentangled solutions discussed above, the relaxation time of the chain is calculated as a hierarchy of timescales. The relaxation time of the correlation blob τ_ξ is still given by Eq. 16. The entanglement strand is a random walk of correlation volumes and relaxes by Rouse motion with time scale τ_e analogous to Eq. 17

$$\tau_e = \tau_\xi \, (N_e/g)^2 \tag{20}$$

where N_e is the number of Kuhn monomers in an entanglement strand, making N_e/g the number of correlation blobs per entanglement strand. The reptation time of the chain (de Gennes 1971; Doi and Edwards 1986; Rubinstein and Colby 2003) is then calculated as for an entangled chain in the melt

$$\tau_{rep} \approx \tau_e \, (N/N_e)^2 \approx \tau_\xi \, (N_e/g)^2 \, (N/N_e)^3 \tag{21}$$

resulting in delayed relaxation of the chain in entangled solutions because it needs to reptate to abandon entanglements. The predicted terminal dynamics of entangled polymer solutions based on Eqs. 3, 4, 19, and 21 are summarized in Table 2 for entangled solutions of neutral polymers in good solvents, neutral polymers in θ-solvents, and polyelectrolyte solutions with no salt. For neutral polymers in good solvent and for polyelectrolyte solutions with no salt, the tube diameter is proportional to the correlation length, and the simple de Gennes scaling works nicely to reduce specific viscosity or diffusion coefficient for different molar mass polymers to universal curves by plotting against c/c^*. That scaling reduction for diffusion coefficient has been demonstrated for neutral polymers in good solvent (Rubinstein and Colby 2003, Fig. 8.9) with the exponent −0.54 expected from Table 1 for $c^* < c < c_e$ and the exponent −1.85 expected from Table 2 for $c > c_e$. Oostwal's diffusion data on sodium polystyrene sulfonate in water (Oostwal et al. 1993) also reduce reasonably well by plotting D vs. c/c_e, with the predicted slopes of 0 expected from Table 1 for $c^* < c < c_e$ and the exponent −1/2 expected from Table 2 for $c > c_e$.

The specific viscosity of polyelectrolyte solutions do show the expected transition from scaling as $c^{1/2}$ in semidilute unentangled solutions to scaling as $c^{3/2}$ in entangled solutions (Fernandez Prini and Lagos 1964; Boris and Colby 1998; Krause et al. 1999; DiCola et al. 2004; Dou and Colby 2006, 2008). However, while c/c^* reduces the specific viscosity data in dilute and semidilute unentangled solutions, it fails to reduce data in entangled solutions either for different molar mass (Krause et al. 1999) or for different effective charge (Dou and Colby 2006). That is because the simple de Gennes scaling expects the entanglement concentration to be proportional to c^*, and Fig. 2 shows that does not apply for polyelectrolyte solutions with no salt. Entanglement in polyelectrolyte solutions is not yet well understood.

On the other hand, for neutral polymers in good solvent, Fig. 2 shows that c_e is proportional to c^*, and the simple c/c^* reduction works very nicely for specific viscosity as shown in Fig. 13a for eight mo-

Table 2 De Gennes scaling predictions of solution structure, scaling predictions for the tube diameter, and reptation model predictions for terminal polymer dynamics in entangled solutions for the three universality classes

	General equation	Neutral in θ-solvent	Neutral in good solvent	Polyelectrolyte with no salt
Scaling exponent	$v \equiv \partial(\log R_{\text{dilute}})/\partial(\log N)$	$v = 1/2$	$v = 0.588$	$v = 1$
Correlation blob size	$\xi \sim N^0 c^{-v/(3v-1)}$	$\xi \sim N^0 c^{-1}$	$\xi \sim N^0 c^{-0.76}$	$\xi \sim N^0 c^{-1/2}$
Polymer size	$R \sim N^{1/2} c^{-(v-1/2)/(3v-1)}$	$R \sim N^{1/2} c^0$	$R \sim N^{1/2} c^{-0.12}$	$R \sim N^{1/2} c^{-1/4}$
Tube diameter	$a \sim \xi$ *	$a \sim N^0 c^{-2/3}$	$a \sim N^0 c^{-0.76}$	$a \sim N^0 c^{-1/2}$
Reptation time	$\tau_{\text{rep}} \sim N^3 c^{3(1-v)/(3v-1)}$ *	$\tau_{\text{rep}} \sim N^3 c^{7/3}$	$\tau_{\text{rep}} \sim N^3 c^{1.6}$	$\tau_{\text{rep}} \sim N^3 c^0$
Terminal modulus	$G_{\text{e}} = \frac{kT}{a^2\xi}$	$G_{\text{e}} \sim N^0 c^{7/3}$	$G_{\text{e}} \sim N^0 c^{2.3}$	$G_{\text{e}} \sim N^0 c^{3/2}$
Polymer contribution to viscosity	$\eta - \eta_{\text{s}} \approx G\tau \sim N^3 c^{3/(3v-1)}$ *	$\eta - \eta_{\text{s}} \sim N^3 c^{14/3}$	$\eta - \eta_{\text{s}} \sim N^3 c^{3.9}$	$\eta - \eta_{\text{s}} \sim N^3 c^{3/2}$
Diffusion coefficient	$D \approx R^2/\tau \sim N^{-2} c^{-(2-v)/(3v-1)}$ *	$D \sim N^{-2} c^{-7/3}$	$D \sim N^{-2} c^{-1.85}$	$D \sim N^{-2} c^{-1/2}$

*For neutral polymers in good solvent and polyelectrolytes with no salt (neutral polymers in θ-solvent differ because of two-parameter scaling)

lar masses of polystyrene in the good solvent toluene (Adam and Delsanti 1983). For neutral polymers in θ-solvent, the simple c/c^* scaling utterly fails (Adam and Delsanti 1984) as expected by the two-parameter scaling presented here (Table 2) since the tube diameter and correlation length have different concentration dependences (Colby and Rubinstein 1990; Rubinstein and Colby 2003). The two-parameter scaling expects
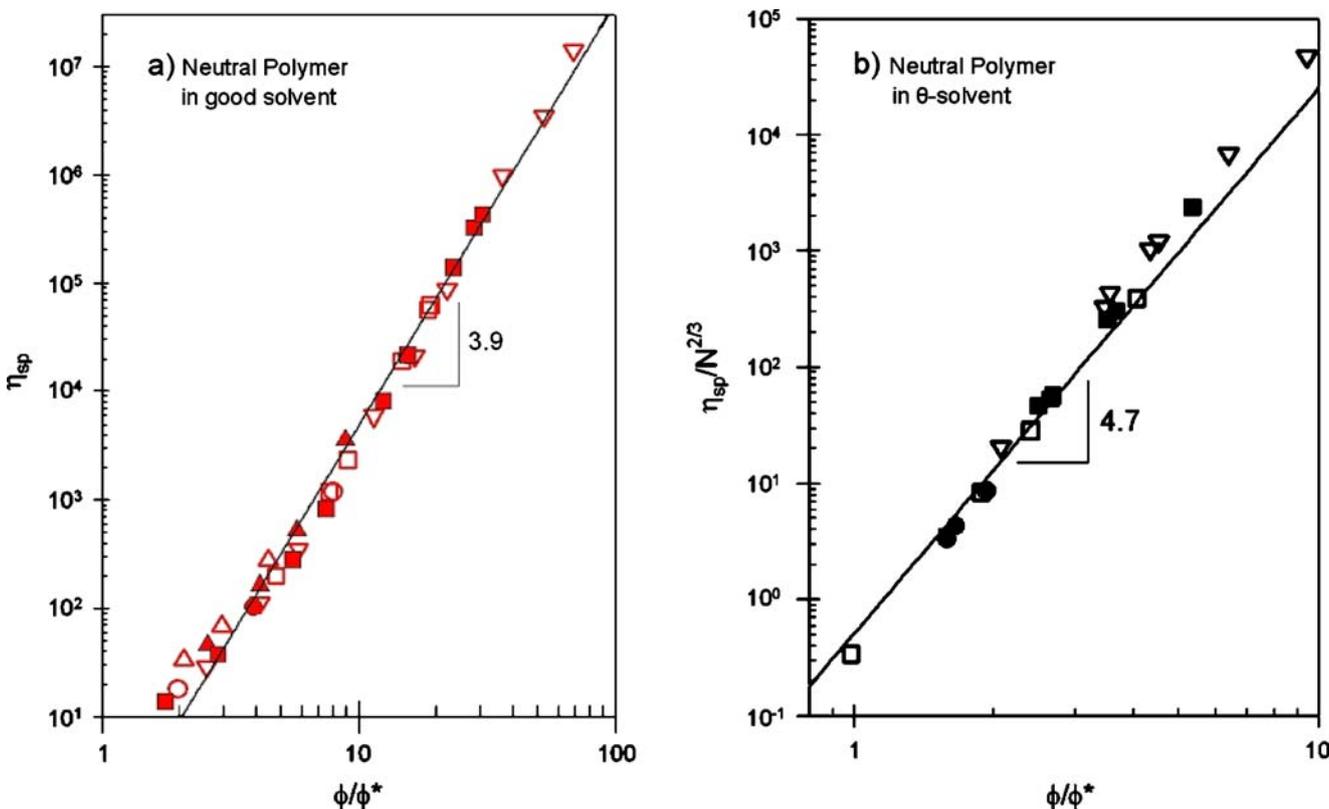
Fig. 13 Concentration dependence of specific viscosity for semi-dilute solutions of various molar mass polystyrene at 35°C. **a** Solutions in the good solvent toluene show that de Gennes simple scaling (de Gennes 1979) works nicely (Adam and Delsanti 1983). **b** Solutions in the θ-solvent cyclohexane need to have specific viscosity divided by $N^{2/3}$ to reduce different molar mass data to a common curve (Adam and Delsanti 1984) as expected by two-parameter scaling (Colby and Rubinstein 1990). *Open triangles* are $M = 174{,}000$; *filled triangles* are $M = 422{,}000$; *open circles* are $M = 1{,}260{,}000$; *filled circles* are $M = 2{,}890{,}000$; *open squares* are $M = 3{,}840{,}000$; *filled squares* are $M = 6{,}770{,}000$; *open inverted triangles* are $M = 20{,}600{,}000$. *Lines* are the expected slopes from Table 2 (following Rubinstein and Colby 2003, Fig. 9.10)

that one needs to divide specific viscosity by $N^{2/3}$ and plot against $c/c*$, which Fig. 13b shows works nicely for four molar masses of polystyrene in the θ-solvent cyclohexane (Adam and Delsanti 1984). Note that in both sets of data in Fig. 13, Adam and Delsanti used $c*$ calculated from radius of gyration, meaning that their $c*$ is actually closer in magnitude to c_e, as discussed above (their lowest specific viscosity in good solvent is 13.8 for $c/c* = 1.8$ using their definition of $c*$).

The two-parameter scaling model expects $\phi_e \sim N^{-3/4}$ in θ-solvent, which has not yet been experimentally tested. Combined with the fact that $\phi* \sim N^{-1/2}$ in θ-solvent, $\phi_e/\phi* \sim N^{-1/4}$ meaning that the semidilute unentangled regime is expected to be vanishingly small for long neutral chains in θ-solvent.

Figure 14 shows oscillatory shear data on entangled solutions of a high molar mass neutral polybutadiene in a near-θ solvent and a good solvent (Colby et al. 1991). For the near-θ solvent, all the concentrations shown are expected to be in the "semidilute θ" regime (see Fig. 5.1 of Rubinstein and Colby 2003) where the thermal blob size is larger than the correlation length, meaning that

the entire chain should have a random walk conformation at the seven concentrations shown, even though dilute solution light scattering and intrinsic viscosity suggest that this high molar mass polybutadiene is slightly swollen by excluded volume ($T = 25°C \approx \theta + 10$ K). A complication with polymer solutions that has not been discussed in this review is that the glass transition temperature (T_g) of the solution changes with concentration. For solutions of high-T_g polymers (such as polystyrene) in low-T_g solvents (such as toluene), this concentration dependence is quite strong (Ferry 1980, Fig. 17-1; Graessley 2008, Fig. 8.18). However, for the solutions in Fig. 14, polybutadiene ($T_g = 174$ K) was dissolved in the solvents dioctylphthalate ($T_g = 185$ K) and phenyloctane ($T_g = 152$ K), so the concentration dependence of T_g is far weaker. The data in Fig. 14 show the entanglement plateau that is very evident for the polymer melt (top curves) gradually diminishes as the concentration is lowered.

Entangled solutions of neutral polymers in good solvent exhibit precisely the scaling de Gennes predicted, with diffusion coefficient and specific viscosity for
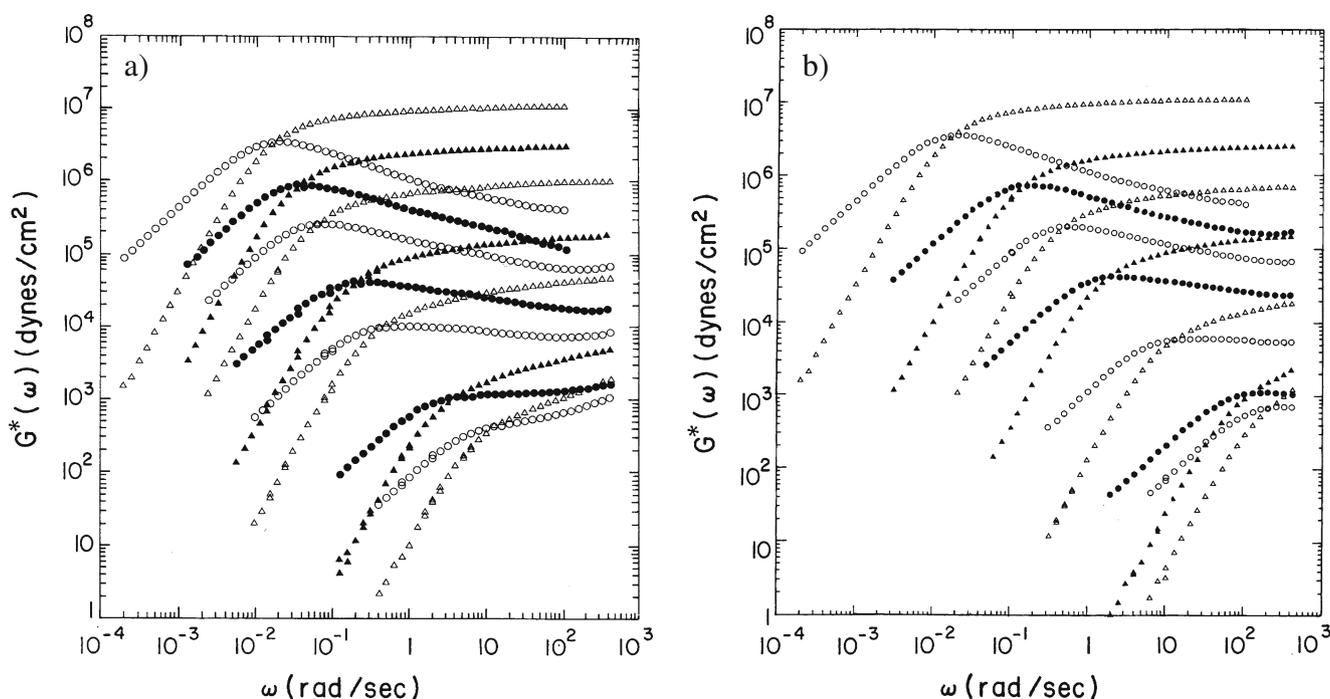
Fig. 14 Oscillatory shear data on neutral polybutadiene $M_w = 925,000$ entangled solutions. **a** Polymer melt and six solutions in the θ-solvent dioctylphthalate at 25°C with volume fraction of polymer from top to bottom $\phi = 1$ ($T_g = 174$ K), $\phi = 0.523$ ($T_g = 181$ K), $\phi = 0.306$ ($T_g = 183$ K), $\phi = 0.157$ ($T_g = 184$ K), $\phi = 0.0806$, $\phi = 0.0308$, $\phi = 0.0214$ ($T_g = 187$ K). For dioctylphthalate, $T_g = 185$ K and $\theta \approx 15°C$, meaning that all six solutions in dioctylphthalate at 25°C are in the "semidilute θ" regime (see Fig. 5.1 of Rubinstein and Colby 2003) and $\phi_e \approx 0.01$, meaning

that all six solutions are entangled. **b** Polymer melt and six solutions in the good solvent phenyloctane at 25°C with volume fraction of polymer from top to bottom $\phi = 1$ ($T_g = 174$ K), $\phi = 0.488$ ($T_g = 157$ K), $\phi = 0.280$ ($T_g = 154$ K), $\phi = 0.140$ ($T_g = 152$ K), $\phi = 0.0621$, $\phi = 0.0274$ ($T_g = 150$ K), $\phi = 0.0214$. For phenyloctane, $T_g = 152$ K and $\phi_e \approx 0.01$, meaning that all six solutions are entangled. Both figures are used with permission from Colby et al. (1991)

different molar masses, different polymers, and different good solvents reduced to common curves when plotted against c/c^*. Entangled solutions of neutral polymers in θ-solvent have an added complication because the tube diameter has a different concentration dependence than the correlation length, but the two-parameter scaling model describes all measurements made thus far. Entangled polyelectrolyte solutions with no salt are not fully understood because we do not yet grasp the effects of charge (and local chain stretching inside the correlation length, see Fig. 4b) on chain entanglement, although the concentration-dependent power laws predicted from the Rouse and reptation models are observed for diffusion coefficient and specific viscosity. Entangled polymer solutions are extremely important for polymer processing operations that require elastic character for stability, such as wet fiber spinning and electrospinning. Electrospinning from semidilute unentangled solutions produces a mixture of fibers and beads (McKee et al. 2004). Electrospinning from entangled solutions of neutral polymers in good solvent produces only fibers, with the fiber diameter increasing with concentration (McKee et al. 2004). Consequently, to make small diameter fibers using electrospinning, it is best to use solutions slightly above the entanglement concentration. Similar conclusions are observed for polyelectrolyte solutions with added salt (McKee et al. 2006) because polyelectrolytes in solutions with considerable salt are in the neutral-polymer-in-good-solvent universality class since screened charge repulsion is quite analogous to excluded volume (Pfeuty 1978; Dobrynin et al. 1995; Dobrynin and Rubinstein 2005). Again, owing to environmental concerns, we expect aqueous solutions to play important roles in future use of polymer solution processing operations like wet fiber spinning and electrospinning.

Conclusion

De Gennes' simple notion of a correlation length that separates semidilute conformations and dynamics into dilute-like inside the correlation volume and melt-like on larger scales works amazingly well to describe both the structure and linear viscoelasticity of solutions of flexible polymers. That statement holds for all three universality classes of polymer solutions. Neutral polymers in good solvent have both excluded volume and hydrodynamic interaction screened at the correlation length. Neutral polymers in θ-solvent just have hydrodynamic interactions screened at the correlation length but also have tube diameter not proportional to corre-

lation length, which complicates their dynamics in entangled solution but in ways that are fully understood. Polyelectrolyte solutions with no salt have electrostatic interactions and hydrodynamic interactions screened at their correlation length, and the same ideas used for neutral polymers then apply to polyelectrolyte solution dynamics.

There are two outstanding problems left to be resolved. The first is that while seemingly perfect for neutral polymers in θ-solvent, the Zimm model does not seem to describe dilute solutions of neutral polymers in good solvent. The presence of excluded volume seems to greatly diminish the hydrodynamic interactions (Hair and Amis 1989; Graessley 2008, pp. 447–450). On a related topic, dilute solutions of polyelectrolytes with no salt have not yet been studied, primarily because c^* is very low and in aqueous solutions exposed to air, there is residual salt that makes study of polyelectrolyte solutions in the low-salt limit challenging (Cohen et al. 1988; Boris and Colby 1998). Dilute solutions of salt-free polyelectrolytes are expected to be interesting because the electrostatic (Debye) screening length has a stronger concentration dependence than the distance between chains, so in dilute solutions with no salt, polyelectrolytes should interact strongly (de Gennes et al. 1976). Also, solutions of strongly solvophobic polyelectrolytes (DiCola et al. 2004; Alexander-Katz and Leibler 2009) behave quite differently and were not discussed in this review.

The second outstanding problem is chain entanglement in polyelectrolyte solutions. While the predicted concentration dependences of diffusion coefficient and specific viscosity are observed in Fig. 15 for entangled polyelectrolyte solutions with no added salt, the entanglement concentration has a very different dependence on chain length than the overlap concentration (Fig. 2). This causes the observed dependences on chain length (Krause et al. 1999) and effective charge (Dou and Colby 2006) to be quite different than expected by the scaling model for entangled polyelectrolyte solutions with no added salt. The scaling theory expects the value of the specific viscosity at the entanglement concentration to be independent of chain length and entanglement concentration and only depend on the square of the number of overlapping strands n defining an entanglement volume

$$\eta_{sp}(c_e) \approx n^2 \qquad (22)$$

which is clearly not observed in Fig. 15a where $\eta_{sp}(c_e) \sim c_e^{-1.76}$ (dashed line) and suggests that $n^2 \sim c_e^{-1.76}$. The scaling theory expects the diffusion coefficient at the entanglement concentration to be
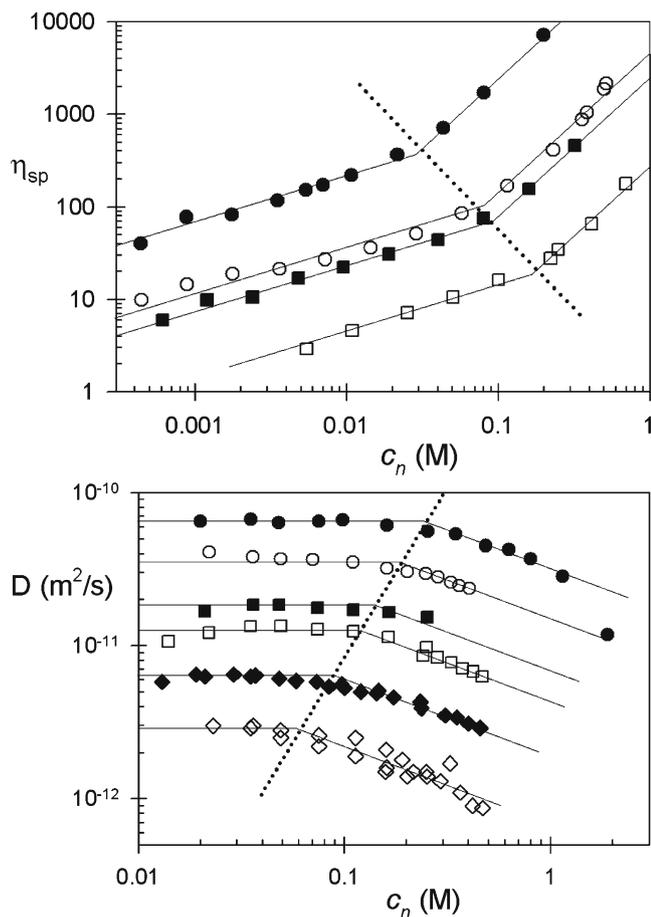
Fig. 15 Concentration dependences of specific viscosity and diffusion coefficient for polyelectrolyte solutions clearly showing the entanglement concentration. **a** Specific viscosity of sodium poly(2-acrylamido-2-methylpropane sulfonate) in water: *filled circles* $M = 1.7 \times 10^6$, *filled squares* $M = 9.5 \times 10^5$ (Krause et al. 1999) and sodium poly(styrene sulfonate) in water: *open circles* $M = 1.2 \times 10^6$ (Boris and Colby 1998), *open squares* $M = 3.0 \times 10^5$ (Fernandez Prini and Lagos 1964). *Solid lines* have the expected slopes of 1/2 and 3/2, *dotted line* has slope -1.76. **b** Diffusion coefficient of sodium poly(styrene sulfonate) in water: *filled circles* $M = 16{,}000$, *open circles* $M = 31000$, *filled squares* $M = 65000$, *open squares* $M = 88{,}000$, *filled diamonds* $M = 177{,}000$, *open diamonds* $M = 354{,}000$ (Oostwal et al. 1993). *Solid lines* have the expected slopes of 0 and $-1/2$, *dotted line* has slope 2.29

inversely related to chain length N and with $c_e \sim n^4/N^2$ (Dobrynin et al. 1995) that leads to:

$$D(c_e) \sim c_e^{1/2} \Big/ n^2 \qquad (23)$$

which is clearly not observed in Fig. 15b where $D(c_e) \sim c_e^{2.29}$ (dashed line) and that is also quite consistent with viscosity, as it suggests $n^2 \sim c_e^{-1.79}$. The facts that (1) the expected concentration dependences of viscosity and diffusion coefficient are clearly observed (Fig. 15) and (2) the entanglement criteria deviate from expectation

in precisely the same manner for viscosity and diffusion suggest that one should not immediately discard the scaling model. Instead, a different criterion for entanglement needs to be understood, with the number of overlapping strands forming an entanglement having a surprising dependence on chain length $n \sim N^{-0.39}$ (Boris and Colby 1998) and the entanglement concentration having a far weaker dependence on N than the expected N^{-2} dependence, with $c_e \sim N^{-0.44}$, quite consistent with both the entanglement concentrations from viscosity shown in Fig. 2 and also the entanglement concentration extracted from the diffusion measurements of Oostwal et al. (1993). Exactly how the strong electrostatic repulsion that acts to stretch the polyelectrolyte locally impacts entanglement remains to be solved and may even lead to a better understanding of entanglements in all solutions. It is indeed remarkable how theory of entangled solutions can describe most observations without a detailed understanding of what an entanglement is!

References

Adam M, Delsanti M (1983) J Phys France 44:1185

Adam M, Delsanti M (1984) J Phys France 45:1513

Agarwal PK, Garner RT, Graessley WW (1987) J Polym Sci, Polym Phys 25:2095

Alexander-Katz A, Leibler L (2009) Soft Matter 5:2198

Berry GC, Fox TG (1968) Adv Polym Sci 5:261

Bohdanecky M, Kovar J (1982) Viscosity of polymer solutions. Elsevier, New York

Bordi F, Cametti C, Colby RH (2004) J Phys: Condens Matt 16:R1423

Bordi F, Cametti C, Tan JS, Boris DC, Krause WE, Plucktaveesak N, Colby RH (2002) Macromolecules 35:7031

Boris DC, Colby RH (1998) Macromolecules 31:5746

Chen SP, Archer LA (1999) J Polym Sci, Polym Phys 37:825

Cohen J, Priel Z, Rabin Y (1988) J Chem Phys 88:7111

Colby RH, Rubinstein M (1990) Macromolecules 23:2753

Colby RH, Fetters LJ, Funk WG, Graessley WW (1991) Macromolecules 24:3873

Colby RH, Boris DC, Krause WE, Dou S (2007) Rheol Acta 46:569

Cotton JP, Nierlich M, Boué F, Daoud M, Farnoux B, Jannink G, Duplessix R, Picot C (1976) J Chem Phys 65:1101

Daoud M, Cotton JP, Farnoux B, Jannink G, Sarma G, Benoit H, Duplessix R, Picot C, de Gennes PG (1975) Macromolecules 8:804

de Gennes PG (1971) J Chem Phys 55:572

de Gennes PG (1976a) Macromolecules 9:587

de Gennes PG (1976b) Macromolecules 9:594

de Gennes PG (1979) Scaling concepts in polymer physics. Cornell University Press, Ithaca

de Gennes PG, Pincus P, Velasco RM, Brochard F (1976) J Phys (Paris) 37:1461

DiCola E, Plucktaveesak N, Waigh TA, Colby RH, Tan JS, Pyckhout-Hintzen W, Heenan RK (2004) Macromolecules 37:8457

Dobrynin AV, Rubinstein M (2005) Prog Polym Sci 30:1049

Dobrynin AV, Colby RH, Rubinstein M (1995) Macromolecules 28:1859

Doi M, Edwards SF (1986) The theory of polymer dynamics. Oxford University Press, New York

Donnan PG, Guggenheim EA (1934) Z Phys Chem 162:364

Dou S, Colby RH (2006) J Polym Sci Polym Phys 44:2001

Dou S, Colby RH (2008) Macromolecules 41:6505

Dragan S, Mihai M, Ghimici L (2003) Eur Polym J 39:1847

Drifford M, Dalbiez JP (1984) J Phys Chem 88:5368

Edwards SF (1966) Proc Phys Soc 88:265

Essafi W, Lafuma F, Baigl D, Williams CE (2005) Europhys Lett 71:938

Fernandez Prini R, Lagos AE (1964) J Polym Sci A-2:2917

Ferry JD (1980) Viscoelastic properties of polymers, 3rd edn. Wiley, New York

Flory PJ, Daoust H (1957) J Polym Sci 25:429

Fuoss RM (1948) J Polym Sci 3:603

Fuoss RM (1951) Disc Faraday Soc 11:125

Fuoss RM, Strauss UP (1948) J Polym Sci 3:246

Geissler E, Mallam S, Hecht AM, Rennie AR, Horkay F (1990) Macromolecules 23:5270

Graessley WW (1974) Adv Polym Sci 16:1

Graessley WW (1980) Polymer 21:258

Graessley WW (2003) Polymeric liquids and networks: structure and properties. Garland Science, New York

Graessley WW (2008) Polymeric liquids and networks: dynamics and rheology. Garland Science, New York

Hair DW, Amis EJ (1989) Macromolecules 22:4528

Hara M, Wu JL, Lee AH (1988) Macromolecules 21:2214

Higgins JS, Benoit HC (1994) Polymers and neutron scattering. Oxford University Press, New York

Higgins JS, Roots JE (1985) J Chem Soc Faraday Trans 81:757

Hodgson DF, Amis EJ (1991) J Chem Phys 94:4581

Johnson RM, Schrag JL, Ferry JD (1970) Polym J 1:742

Jousset S, Bellissent H, Galin JC (1998) Macromolecules 31:4520

Kaji K, Urakawa H, Kanaya T, Kitamaru R (1988) J Phys France 49:993

Katchalsky A (1971) Pure Appl Chem 26:327

Kim MW, Peiffer DG (1988) Europhys Lett 5:321

King JS, Boyer W, Wignall GD, Ullman R (1985) Macromolecules 18:709

Krause WE, Tan JS, Colby RH (1999) J Polym Sci, Polym Phys 37:3429

Kulicke WM, Kniewske R (1984) Rheol Acta 23:75

Kulicke WM, Griebel Th, Bouldin M (1991) Polymer News 16:39

Lodge TP, Schrag JL (1982) Macromolecules 15:1376

Marcus RA (1955) J Chem Phys 23:1057

McKee MG, Wilkes GL, Colby RH, Long TE (2004) Macromolecules 37:1760

McKee MG, Hunley MT, Layman JM, Long TE (2006) Macromolecules 39:575

Nierlich M, Boue F, Lapp A, Oberthur R (1985) J Phys (Paris) 46:649

Nierlich M, Williams CE, Boué F, Cotton JP, Daoud M, Farnoux B, Jannink G, Picot C, Moan M, Wolff C, Rinaudo M, de Gennes PG (1979) J Phys (Paris) 40:701

Onogi S, Masuda T, Kitagawa K (1970) Macromolecules 3:109

Onogi S, Kimura S, Kato T, Masuda T, Miyanaga N (1966) J Polym Sci C15:381

Oosawa F (1971) Polyelectrolytes. Marcel Dekker, New York

Oostwal MG, Blees MH, de Bleijser J, Leyte JC (1993) Macromolecules 26:7300

Pearson DS (1987) Rubb Chem Tech 60:439

Pedersen JS, Schurtenberger P (2004) J Polym Sci, Polym Phys 42:3081

Pfeuty P (1978) J Phys (Paris) Colloq C2:149

Plucktaveesak N, Konop AJ, Colby RH (2003) J Phys Chem B 107:8166

Richter D, Farago B, Butera R, Fetters LJ, Huang JS, Ewen B (1993) Macromolecules 26:795

Rosser RW, Nemoto N, Schrag JL, Ferry JD (1978) J Polym Sci, Polym Phys 16:1031

Rouse PE (1953) J Chem Phys 21:1272

Rubinstein M, Colby RH (2003) Polymer physics. Oxford University Press, New York

Semenov AN (1988) J Phys France 49:175, 1353

Strauss UP, Smith EH (1953) J Am Chem Soc 75:6186

Takahashi A, Kato N, Nagasawa M (1970) J Phys Chem 74:944

Takahashi Y, Yamaguchi M, Sakakura D, Noda I (1991) Nihon Reoroji Gakkaishi 19:39

Takahashi Y, Iio S, Matsumoto N, Noda I (1996) Polym Int 40:269

Takahashi Y, Sakakura D, Wakutsu M, Yamaguchi M, Noda I (1992) Polym J 24:987

Tao H, Huang C, Lodge TP (1999) Macromolecules 32:1212

Teraoka I (2002) Polymer solutions. Wiley, New York

Terayama H, Wall FT (1955) J Polym Sci 16:357

van't Hoff JH (1887) Z Physik Chemie 1:481

Xu Z, Qian R, Hadjichristidis N, Fetters LJ (1984) J China Univ Sci Tech 14:228

Zebrowski BE, Fuller GG (1985) J Rheol 29:943

Zimm BH (1956) J Chem Phys 24:269